Available online at www.sciencedirect.com
SCIENCE DIRECT®
Applied Surface Science 230 (2004) 393–397
applied surface science
www.elsevier.com/locate/apsusc

Nanoscale islands and color centers in porous anodic alumina on silicon fabricated by oxalic acid

Y.F. Mei[a,*], G.G. Siu[a], G.S. Huang[b], X.L. Wu[b]

[a]Department of Physics and Materials Science, City University of Hong Kong, Kowloon, Hong Kong, PR China
[b]National Laboratory of Solid State Microstructures and Department of Physics, Nanjing University, Nanjing 210093, PR China

Received in revised form 3 March 2004; accepted 3 March 2004

Available online 17 April 2004

Abstract

Anodic oxidation of Al film on silicon substrate in oxalic acid is investigated through the *j–t* curves and its photoluminescence (PL). Their growth is analyzed with three typical stages according to *j–t* curve, which is agreed with the growth of nanoscale SiO_2 islands at the interface between Al film and Si substrate. The violet and blue peaks of PL were due to F^+ and F centers, respectively. The evolvement from F^+ to F centers during the late stage of anodization was revealed by the PL behavior at different stage.

PACS: 78.55.−m; 78.55.Mb; 61.72.Ji; 82.80.Fk

Keywords: Photoluminescence; Porous materials; Color centers; Electrochemical methods

1. Introduction

Porous anodic alumina (PAA), a porous oxide membrane formed on aluminum, is very useful as template in fabrication of nanomaterials and nanostructures [1,2], such as carbon nanotube (CNT) [3], monocrystal Ag nanowires [4], and CdS nanowires [5]. Nanostructures and their array are synthesized on various substrates with PAA template such as Si substrate [6–8] for nanoelectrics, on glass substrate with a conductive tin doped indium oxide layer [9] for display and on thin film such as SiGe [10] or SiO_2 [11] on silicon substrate for nano-optoelectronics. Experimental and theoretical progress has been made to elucidate anodic oxidation of PAA, important for improving nanostructure fabrication, especially when PAA template is converted to other substrate.

The properties of PAA are affected by many anodization variables (e.g. voltage, temperature, and electrolyte concentration). Among its properties, the optical one not only characterizes PAA but also decides its potential application in light source array [11] and nanolaser [12], etc. PAA can emit light when excited with UV radiation. This photoluminescence (PL) is susceptible to its environment because of its porous structure and amorphous morphology [13]. PL was attributed some impurity at first [14]. Recently the singly ionized oxygen vacancies (F^+ center) were identified as PL centers through electron paramagnetic resonance (EPR) [15]. Analyses of PL peaks showed

* Corresponding author. Tel.: +852-2194-2824; fax: +852-2788-7830.
E-mail address: meiyongfeng@nju.org.cn (Y.F. Mei).

0169-4332/$ – see front matter © 2004 Elsevier B.V. All rights reserved.
doi:10.1016/j.apsusc.2004.03.006

that there are two different defects (F and F^+ centers) in PAA. The asymmetry of PL bands was attributed to the inhomogeneity in defect distribution [16]. However, for the identified PL mechanism of PAA, it is necessary to reveal the details of growth process of PAA and its relationship with optical property.

In this work, PAA on Si substrate are prepared electrochemically in oxalic acid. Its growth is monitored through the dependence of current density on time (j–t curves) and PL, showing defect (color center) variations corresponding to different anodization stages. The conversion from F^+ to F was responsible for the PL changes during the late growth stage. The evolvement of defects is helpful to understand the growth process, PL mechanism, and self-organized mechanism.

2. Experiments

Aluminum film (99.99%) with thickness 440 nm was deposited on the p-type, 0.5 Ω cm, and ⟨1 0 0⟩ -oriented silicon substrate using electron beam evaporation. The vacuum chamber was maintained under a pressure of 2.5×10^{-6} Pa. The accelerating voltage of the electron beam is held essentially constant ∼10 kV and electron gun current is 0.5 A. The as-deposited Al film had smooth and compact surface, and the Al film on Si substrate (Al/Si) was directly used as an anode with a platinum plate as a cathode. Several Al/Si were anodized in 0.5 M oxalic acid under a constant DC voltage of 40 V at room temperature. The growth can be monitored with j–t curves. The surface of the fabricated PAA was checked by a JEOL JSM-6300 scanning electron microscope (SEM) and PL was measured at room temperature by a Fluoro-Max-2 photospectrometer. AFM measurements were carried out on nanoscope IIIa Digital Instruments.

3. Results and discussion

Fig. 1 shows the j–t curves for anodization of PAA on Si substrate respectively in 0.5 M acid solutions at room temperature. In Fig. 1a, typical stages are included by three anodization processes, corresponding to (I) the initiation of nanopores, (II) the stable growth of channels in PAA on Si substrate, and (III)

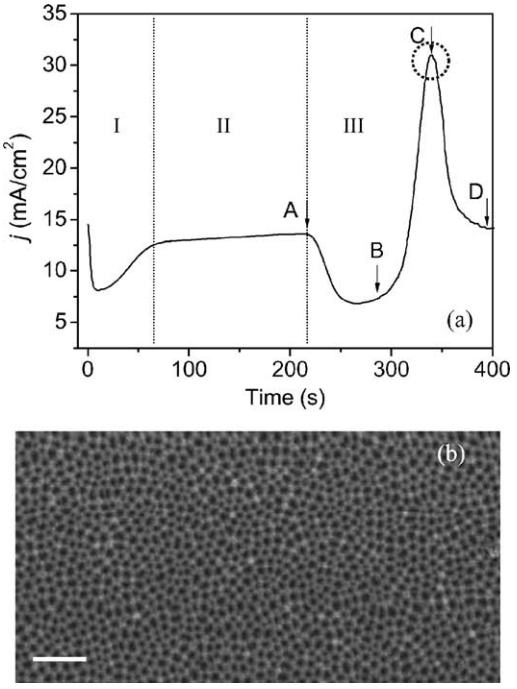

Fig. 1. The j–t curves for anodization of PAA film on Si substrate in (a) 0.5 M oxalic acid solution, (b) is the planar SEM image of PAA template on silicon substrate formed in oxalic acid (the scale bar is 500 nm).

the transition of anodization from aluminum film to silicon substrate.

According to the existing point of view, anodization processes from aluminum to silicon substrate. In stage I immediately after switching on the anodic bias, the current density (j) decreases for the existence of natural thin oxide layer on the aluminum film. When the natural oxide layer is dissolved, the current density increases and reaches a stable anodization in stage II, when oxide growth and dissolution are balanced. When aluminum is going to be exhausted, the current density declines at the beginning of stage III because anodization of silicon substrate starts at the same time. In stage III, the alumina dissolution reduces resistance since no more oxide growth without residual Al [17]. Silicon oxide formed in the anodization of silicon substrate, on the contrary, increases the resistance of substrate. The competition of the two generates a minimum in the surface resistance, which increases later. Correspondingly the current density reaches a maximum at the position C (the dotted circle in Fig. 1a).

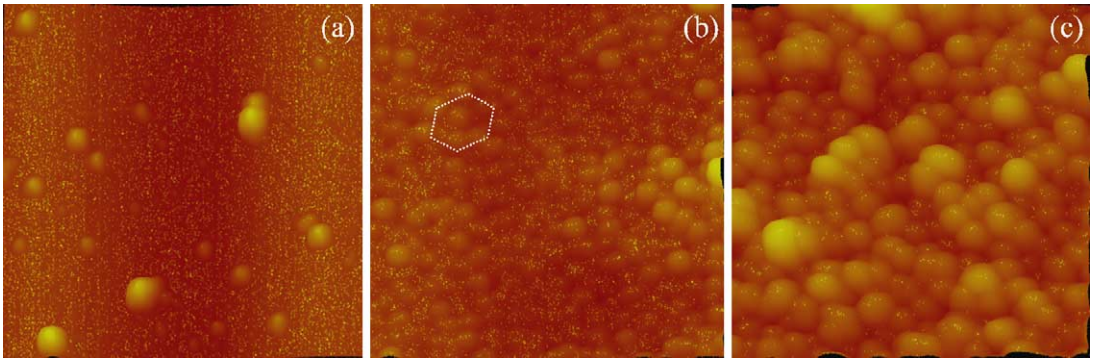

Fig. 2. Three images of silicon dioxide nanoscale islands arrays formed with different anodization time according to (a) position B, (b) position C, and (c) position D in *j–t* curve (Fig. 1a). (The size of each image is 1.5 μm × 1.5 μm).

The SEM image of the sample anodized in 0.5 M oxalic acid solution is shown in Fig. 1b. A uniform nanopores array can be observed. Owing to small grain (100–1000 nm) [8], their arrangement has lower order than PAA on bulk Al [2].

From the above, the growth in stage III seems complicated because of the existance of anodization of both Al film and Si substrate. It is necessary to reveal it because of potential applications such as nanoscale islands growth and efficient deposition of nanowire into nanopores of templates. According to A, B, C, and D position along the *j–t* curve in oxalic acid (Fig. 1a), four samples are obtained, which are expected to monitor the anodization process at the interface between Al film and Si substrate. These samples are divided into two groups.

The first groups of A, B, C, D samples were immersed into a 5 wt.% phosphoric acid solution at 27 °C for long time till no alumina existed on the surface of Si substrate even aluminum. Their surfaces are then studied by AFM for possible silicon oxide and the results are shown in Fig. 2. There is no silicon oxide on the surface of sample A (not shown). A few silicon oxide islands are formed in sample B as shown in Fig. 2a). More silicon oxide islands, 15–20 nm in diameter and 5–10 nm in height, appear in sample C and they are form nanoscale island array with local hexagonal order as shown in Fig. 3B (note the dotted hexagon). This feature is useful in silicon-based nano-electronics and nano-optoelectronics. These silicon oxide islands become larger and pile up with further anodization, as shown by sample D (Fig. 3C). Fourier-transform infrared (FTIR) absorption spectra identify the silicon oxide with silicon dioxide (SiO_2).

The PL spectra of these samples in the second group, which remain unchanged, are compared as shown in Fig. 3A under excitation with the 290 nm line of a Xe lamp. They contain two peaks: violet peak (>3 eV) and blue peak (<3 eV) as follows:

Sample	New (nm)	Violet (nm) (>3 eV)	Blue (nm) (<3 eV)
A	–	337	414
B	–	377 ↑	441
C	332 w	390 ↑	457
D	345 ↓	402 ↓	476 ↓

The arrow denotes the intensity change and w denotes weak band. The red shift of both violet and blue peaks with prolonged anodization may be caused by the internal stress that increases with anodization. The internal stress at the interface between Al film and Si substrate may be further increased by the expansion of SiO_2 from silicon anodization. As a possible cause, the change in the local structure during anodization may induce a red shift, which need further exploration.

The violet peak intensities dramatically increase from sample A to C but weaken in D. The blue peak has little enhancement from A to C and weakens in D. It shows two different types of PL center owing to the incoherence of two peaks with anodization time. The oxygen vacancy without electron (F^{++} center) can be also negated for its instability [13]. So it may be assumed that the F and F^+ defect centers which are

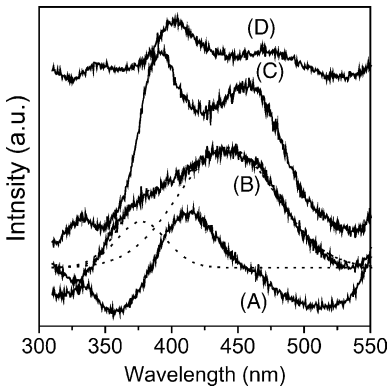

Fig. 3. The PL spectra of the PAA films on Si substrate (samples A, B, C, D corresponding to A, B, C, D in *j–t* curve) obtained in oxalic acid.

responsible for the PL. As explained by others [15,16,18] the blue peak is related to the F^+ centers. Then the violet peak is due to F defect center. Its first excited state is at ~3.0 eV in crystalline alumina [19]. We considered the origin of the new peaks as being due to impurity, which is explained later.

Therefore, PL variation shows the change of the concentration of color centers at late stage of anodization. Analyzed according to the PL changes, it can be deduced that the concentration of F centers increases with the prolonged anodization time and that of F^+ centers changes little. In sample D, both of them decrease considerably.

The variation in the concentration of defect centers is affected by the Al_2O_3(Al)/Si interface for the change of PL behavior during the last stage. The stage III begins with remaining thin Al layer.The aluminum film is almost consumed which allows oxygen anions passing through to oxidize silicon [20,21]. SiO_2 (from B to D) on the interface increases resistance for migrating anions so that anions start to assemble on the Al_2O_3/Si interface. The conversion of F^+ to F is hence enhanced [22]:

$$F^+ + e \rightarrow F \quad (1)$$

with electron supplied from anions (such as OH^-, O^{2-}, which come from acid or even water). The intensity of the violet peak related to F center increases from A to C, reflecting the conversion shown in Eq. (1). The intensity of blue peak have little change because the loss of F^+ is compensated by its production by the anodization of the incompletely oxidized alumina on the pore wall with anions [8,23]. At C of the maximum current density, the generation and the consumption of F^+ center achieve equilibrium and both F and F^+ give strong PL. When further anodization, F^+ center decreases since no more incompletely oxidized alumina available in the pore wall and F center is also reduced since alumina continues to dissolve [20]. PAA on Si substrate produces weak PL as shown by sample D. So the transition $F^+ \rightarrow F$ in regime III may be due to the passivating behavior of the non-porous SiO_2 layer which acts as an electron barrier, so that the main part of the applied voltage drops across the SiO_2 layer and electron enhancement occurs in the alumina.

From the above, the interface plays an important role in PL behavior. Another interesting is their PL excitation (PLE) as shown in Fig. 4. The PLE spectra monitored at violet and blue peaks for sample C are identical to that of sample B (Fig. 4a). Shi et al. [19] showed the relation of the energy level between the dye and PAA. Electron excited in PAA transfer from conductive band to oxide layer of surface and energy transfer from excited electrons to absorbed dye molecule. However, we could not observe the peak of PL

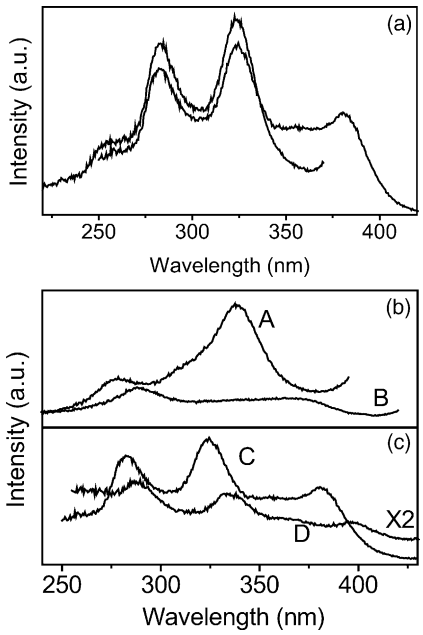

Fig. 4. (a) The PLE spectra of sample C monitored at violet (390 nm) (up) and blue (460 nm) (down) peaks in PL spectra. The PLE spectra of (b) sample A and B, (c) sample C and D, monitored at blue peaks in PL spectra.

excitation near 220 nm in these samples, which corresponds to the band energy level in alumina. Lee and Crawford reported the evidence of carrier release from impurity traps [24]. In current results, the behaviors of PLE (Fig. 4b and c) dramatically changed at the last stage of anodization. So it is feasible that the PLE originated from the impurity level, which is influenced by its environment depending on the anodization condition.

4. Conclusion

The growth of PAA on Si substrate is analyzed with three typical stages according to the *j–t* curve, which is agreed with the growth of nanoscale SiO_2 islands at the interface between Al film and Si substrate. Oxygen vacancies with one electron (F^+ center) and two electrons (F center) are responsible for blue and violet peaks of their PL. The evolvement from F^+ to F centers during the late stage of anodization was revealed by the PL behavior with a series of samples.

Acknowledgements

One of the authors (Mei) thanks Mr. M. K. Tang and Dr Amy X. Y. Lu for kind help about experiments. This work was also supported by the Grants (Nos. 10225416 and BK2002077) from the Natural Science Foundations of China and JiangSu province.

References

[1] R. Parthasarathy, C.R. Martin, Nature 369 (1994) 298.
[2] H. Masuda, K.S. Fukuda, Science 268 (1995) 1466.
[3] J. Li, C. Papadopoulos, J.M. Xu, Nature 402 (1999) 253; J. Sang, J.S. Lee, Appl. Phys. Lett. 75 (1999) 2047.
[4] J. Zhang, X. Wang, X. Peng, L. Zhang, Appl. Phys. A 75 (2002) 485.
[5] D. Routkevitch, T. Bigioni, M. Moskovits, J.M. Xu, J. Phys. Chem. 100 (1996) 14037; H.Q. Cao, Y. Xu, J.M. Hong, H.B. Liu, G. Yin, B.L. Li, C.Y. Tie, Z. Xu, Adv. Mater. 13 (2001) 1393.
[6] H. Masuda, K. Yasui, Y. Sakamoto, M. Nakao, T. Tamamura, K. Nishio, Jpn. J. Appl. Phys. 40 (2001) L1267; S. Shingubara, O. Okino, Y. Sayama, H. Sakaue, T. Takahagi, Solid-State Electron. 43 (1999) 1143.
[7] W.C. Hu, D.W. Gong, Z. Chen, L.M. Yuan, K. Saito, C.A. Grimes, P. Kichambare, Appl. Phys. Lett. 79 (2001) 3083.
[8] Y.F. Mei, X.L. Wu, X.F. Shao, G.S. Huang, G.G. Siu, Phys. Lett. A 309 (2003) 109.
[9] S.Z. Chu, K. Wada, S. Inoue, S.I. Todoroki, Chem. Mater. 14 (2002) 266.
[10] J. Rappich, Solid-State Electron. 45 (2001) 1465.
[11] J.P. Zou, Y.F. Mei, J.K. Shen, J.H. Wu, X.L. Wu, X.M. Bao, Phys. Lett. A 301 (2002) 96.
[12] X.F. Duan, Y. Huang, R. Agarwal, C.M. Lieber, Nature 421 (2003) 241.
[13] J.H. Wu, X.L. Wu, N. Tang, Y.F. Mei, X.M. Bao, Appl. Phys. A 72 (2001) 735.
[14] Y. Yamamto, N. Baba, S. Tajima, Nature 289 (1981) 572.
[15] Y. Du, W.L. Cai, C.M. Mo, J. Chen, L.D. Zhang, X.G. Zhu, Appl. Phys. Lett. 74 (1999) 2951.
[16] G.S. Huang, X.L. Wu, Y.F. Mei, X.F. Shao, G.G. Siu, J. Appl. Phys. 93 (2003) 582.
[17] N. Kouklin, L. Menon, A.Z. Wong, D.W. Thompson, J.A. Woollam, P.F. Williams, S. Bandyopadhyay, Appl. Phys. Lett. 79 (2001) 4423.
[18] W. Chen, H.G. Tang, et al., Appl. Phys. Lett. 67 (1995) 317.
[19] Y.L. Shi, J. Wang, H.L. Li, Appl. Phys. A 75 (2002) 423.
[20] G.E. Thompson, Thin Solid Films 297 (1997) 192.
[21] V.P. Parkhutik, V.I. Shershulsky, J. Phys. D: Appl. Phys. 25 (1992) 1258.
[22] G.J. Pogatshnik, Y. Chen, B.D. Evans, IEEE Trans. on Nucl. Sci. NS-34 (1987) 1709.
[23] Y.F. Mei, X.L. Wu, X.F. Shao, G.G. Siu, X.M. Bao, Europhys. Lett. 62 (2003) 595.
[24] K.H. Lee, J.H. Crawford, Phys. Rev. B 19 (1979) 3217.